Effects of cyclic ageing frequencies on the ageing and mechanical behaviour of adhesive materials

Experimental analysis and numerical study

Moazzami, M.; Akhavan-Safar, A.; Ayatollahi, M.R.; Poulis, Johannes A.; da Silva, L.F.M.; Teixeira De Freitas, S.

DOI
10.1016/j.marstruc.2024.103662

Publication date
2024

Document Version
Final published version

Published in
Marine Structures

Marine Structures 98 (2024) 103662

Contents lists available at ScienceDirect

Marine Structures

journal homepage: www.elsevier.com/locate/marstruc

Effects of cyclic ageing frequencies on the ageing and mechanical behaviour of adhesive materials: Experimental analysis and numerical study

M. Moazzami [a,*], A. Akhavan-Safar [b], M.R. Ayatollahi [a], Johannes.A. Poulis [c], L.F.M. da Silva [d], S. Teixeira De Freitas [c]

[a] *Fatigue and Fracture Research Laboratory, Center of Excellence in Experimental Solid Mechanics and Dynamics, School of Mechanical Engineering, Iran University of Science and Technology, Tehran, Iran*
[b] *Institute of Science and Innovation in Mechanical and Industrial Engineering (INEGI), Porto, Portugal*
[c] *Aerospace Structures and Materials, Faculty of Aerospace Engineering, Delft University of Technology, GB Delft, the Netherlands*
[d] *Department of Mechanical Engineering, Faculty of Engineering, University of Porto, Portugal*

A R T I C L E I N F O

Keywords:
Cyclic aging
Epoxy adhesive
Fick's law
Moisture absorption
Aging frequency

A B S T R A C T

In marine structures adhesive joint structures are often exposed to cyclic conditioning where the ambient humidity changes cyclically during their service. Though some comprehensive studies on the aging of adhesives exist, these researches mainly focus on monotonic aging conditions where the adhesive joints are exposed to a wet condition continuously for a long time. However, the few investigations performed on the cyclic moisture absorption of adhesive materials show that the parameters obtained in monotonic aging conditions are not suitable for estimation of the aging behaviour of adhesive exposed to alternating humidity. An important question that can arise is whether or not this frequency affects the mechanical behaviour of adhesive joints under cyclic aging condition. In this investigation bulk dogbone and square samples were manufactured, subjected to cyclic aging conditions with four different aging frequencies and tested. The results show that the moisture diffusion constant of adhesives exposed to higher aging frequencies increase more than those exposed to lower aging frequency conditions. In addition, the moisture content only affects the degradation of strength and stiffness of the tested adhesives in different aging frequencies.

1. Introduction

Environmental factors such as moisture and temperature can dramatically degrade the mechanical properties of polymer adhesives in marine structures [1–6]. Moisture affects the mechanical properties of the adhesive, and the substrate (when composite substrates are included) [7–10], and the interface between the adhesive and the substrate [11–16]. Scientists have categorized the effects of moisture diffusion into adhesives into reversible (swelling [17] and plasticization [18]) or irreversible (oxidation and hydrolysis [19]) processes. Some investigators [20–22] showed how water molecules bond chemically with the polymeric chains.

Most of the moisture diffusion models are based on the absorbed moisture weight after different exposure times. In most polymers

* Corresponding author.
E-mail address: mostafamoazzemi.70@gmail.com (M. Moazzami).

https://doi.org/10.1016/j.marstruc.2024.103662
Received 19 November 2023; Received in revised form 29 January 2024; Accepted 23 June 2024
Available online 8 July 2024

the moisture diffuses according to Fick's law [23]. However, in some other cases, more complex models have been observed [24]. In addition, Mubashar et al. [25] reported a dual Fickian model for moisture diffusion in an epoxy.

Some authors have studied the variation in mechanical properties of bulk adhesives as a result of monotonous [26] and absorption-desorption aging [27]. Other scientists have investigated the effects of moisture uptake in adhesives as part of a bonded joint [28]. They have reported that the moisture diffusion rate at the interface region is significantly higher than through the adhesive [28]. According to the literature [29] water diffusion at the interface region depends on the substrate surface preparation. Residual stresses caused by swelling in the adhesive can also significantly affect the mechanical performance of adhesive joints [30]. Environmental effects on the performance of adhesive joints have been reviewed more widely in literature [31–34]. Accordingly the behavior of aged adhesive joints strongly depends on the adhesive's chemical formulation, type of surface preparation, curing process, and other environmental conditions such as temperature [34].

Despite extensive studies on the monotonous (continuous) aging of adhesives and bonded joints, however, in practice, bonded structures are often exposed to changing humidity conditions, where the aging-drying cycle is repeated several times in service. Some researchers [35–40] studied the effects of cyclic aging on the moisture diffusion constant and the mechanical properties of adhesive. It was shown that with increasing the aging cycles, the moisture absorption and desorption rate, respectively during the wetting and drying process increases. In addition, the achieved results show that the sensitivity of the tensile strength and elastic modulus decrease with the number of aging cycles [35]. The few studies conducted on the cyclic aging of adhesive joints show that the behaviour of adhesive joints under monotonic aging is completely different from that under cyclic aging conditions. One of the most important parameters in cyclic aging condition is the aging frequency. This parameter can be completely different during the service time of adhesive joints exposed to cyclic aging. This study delves into the impact of aging frequency on the mechanical performance of adhesive joints within a cyclic aging environment. It addresses a notable gap in current research, focusing on the specific effects of cyclic aging conditions with varying frequencies on the mechanical and moisture diffusion behavior of epoxy adhesive—an aspect that has garnered limited attention in existing literature. The paper explores the intricate relationship between aging frequency and the mechanical and moisture diffusion behaviour of epoxy adhesive under cyclic aging conditions. For this purpose, some bulk specimens made of epoxy adhesive were made and exposed to cyclic aging with different frequencies and tested experimentally. Based on these experimental results the effect of aging frequency on the adhesive's mechanical behavior was analysed.

2. Basic theories

In order to analyse the moisture diffusion in polymers, several models have been developed by researchers. The most common and simplest moisture diffusion model is Fick's law [41]. Fick's law can be employed for moisture uptake modeling in most epoxy adhesives. During the moisture diffusion process in polymers, water molecules occupy the free spaces between the polymeric chains and some of them are chemically bonded, turning into bound water. According to Fick's law the variation of the moisture concentration for a large plate during water exposure can be obtained as follows [41]:

$$\frac{\partial C}{\partial t} = D\left(\frac{\partial^2 C}{\partial x^2}\right) \tag{1}$$

where C is the moisture concentration, t is the exposure time, D is diffusion coefficient, and x is the moisture diffusion direction. By integrating the moisture distribution equation over the absorbent plate thickness (h), the instantaneous moisture uptake (M_t) during the absorption can be calculated using the following relation [41].

$$\frac{M_t}{M_m} = \left[1 - \frac{8}{\pi^2}\sum_{n=0}^{\infty}\frac{1}{(2n+1)^2} exp\left(-\frac{(2n+1)^2\pi^2 D}{h^2}t\right)\right] \tag{2}$$

where M_m is the moisture content in saturation condition. Eq. (2) is suitable for monotonous moisture diffusion of the specimens that are initially dried. However, in cyclic aging conditions, the moisture remaining from previous cycles should be considered in the next cycle. During the cyclic aging, with the presence of initial moisture from previous cycles, the instantaneous moisture content during the absorption process can be calculated by the equation below [41]:

$$M_t = \left[1 - \frac{8}{\pi^2}\sum_{n=0}^{\infty}\frac{1}{(2n+1)^2} exp\left(-\frac{(2n+1)^2\pi^2 D}{h^2}t\right)\right] \times (M_m - M_r) + M_r \tag{3}$$

where M_r is the presence of the initial moisture content that remained from the previous cycles. It should be noted that in the first absorption process M_r is equal to zero. To model the moisture content during the desorption process the corresponding Fick's law gives instantaneous moisture content based on the following formula [36]:

$$M_t = \left[\frac{8}{\pi^2}\sum_{n=0}^{\infty}\frac{1}{(2n+1)^2} exp\left(-\frac{(2n+1)^2\pi^2 D_d}{h^2}t\right)\right] \times (M_m - M_r) + M_r \tag{4}$$

where D_d is the diffusion constant of the desorption process. In Eq. (4), M_r is minimum fractional retained moisture after the desorption process and M_m is the maximum moisture uptake when the desorption process starts. The diffusion constant (D and D_d) in absorption and desorption process, can be measured from the initial slope of the moisture uptake curve using the following equation:

$$D = \pi \left(\frac{h}{4M_m} \right)^2 \left(\frac{M_2 - M_1}{\sqrt{t_2} - \sqrt{t_1}} \right)^2 \quad (5)$$

3. Experimental procedure

3.1. Material

A two-component epoxy-based adhesive, Araldite 2011, Huntsman, Basel, Switzerland, was used in this study. The adhesive was mixed with a weight ratio of 100/80 (resin/hardener) using a centrifuge mixing machine, SpeedMixer DAC 150^{TM} (Hauschild, Hamm, Germany), for 2 min at 2300 rpm. After mixing, the adhesive bulk plates were manufactured by curing the adhesive mixture between two thick glass plates coated with a release agent. In order to control the thickness of the adhesive plates, 1 mm thick metal spacers coated by a release agent were used. The adhesive plates were cured for 40 min at 80 °C according to the technical datasheet. Fig. 1 shows the adhesive plate before and after curing.

These adhesive plates were used to make squared and dogbone shaped bulk specimens. These specimens were used in gravimetric and tensile tests, respectively. Table 1 reports the unaged properties of the Araldite 2011 adhesive obtained from tensile tests of dogbone specimens.

3.2. Geometry of the specimens

Square and dogbone bulk specimens were cut out of the adhesive plates. The squared plates were used for the measurement of moisture diffusion parameters in different aging cycles. Dogbone adhesive specimens were used to measure the variation of tensile strength and elastic modulus of cyclically aged adhesive. The geometries of the tested bulk specimens are shown in Fig. 2.

The dimensions of the dogbone specimens are in accordance with the mini dogbone specimens proposed and used by Costa et al. [42].

3.3. Aging process

In various industrial sectors, such as marine structures, adhesive joints undergo cyclic aging due to environmental conditions. The aging frequency varies across different service conditions; for example, offshore structures experience long-duration aging cycles, while small boats may endure high-frequency aging cycles. To explore the impact of aging frequency on the cyclic aging of bonded structures, the manufactured bulk specimens (both the square and dogbone samples) were subjected to four different aging frequencies to analyse the effect of aging frequency on the mechanical response of the tested adhesives. Afterwards, the cyclically aged samples were exposed to a continuous aging condition until saturation.

Table 2 shows the details of the 4 different aging frequencies. As can be seen in Table 2, the total duration of the cyclic aging process was 63 or 65 days, which can be considered constant for all of aging process. This error is unavoidable because of aging cycle duration and number of aging cycles.

After the cyclic aging, the specimens were continuously immersed in distilled water to reach the saturation level. In addition, extra specimens, which were not exposed to cyclic aging, were immersed continuously in distilled water until saturation. The schematic of applied cyclic aging and the final moisture absorption process are illustrated in Fig. 3a.

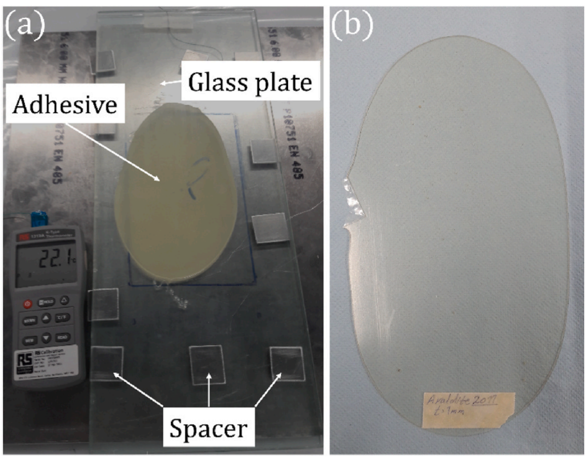

Fig. 1. Adhesive plate before (a), and after curing (b).

Table 1
Physical and mechanical properties of the unaged adhesive.

Property	Value	Unit
Elastic modulus	1550	MPa
Tensile strength	35	MPa
Density	1.05	g/cm^3
Viscosity at 25°C	30–45	Pas

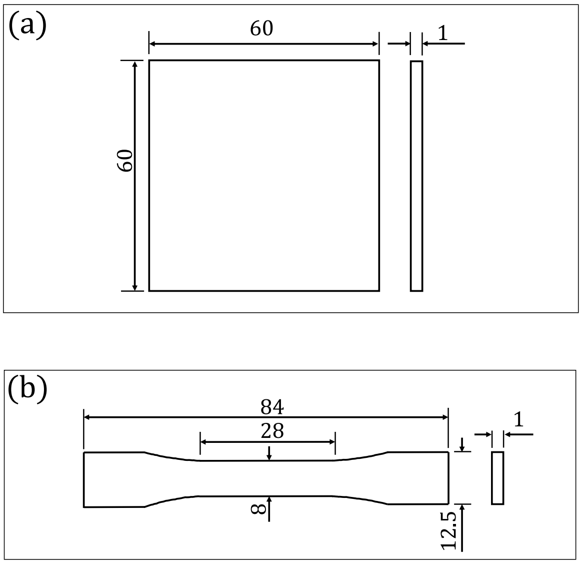

Fig. 2. Geometry of gravimetric (a), and dogbone (c) specimens (dimensions in mm and not to scale).

Table 2
Cyclic aging details.

Process No. absorption-desorption	Absorption time (day)	desorption time (day)	Aging cycles	Total aging time (day)
34–29	34	29	1	63
14–7	14	7	3	63
8–5	8	5	5	65
5–2	5	2	9	63

The temperature of the aging chamber for all the considered aging procedures was set to 25 ± 1 °C. The bulk square and dogbone specimens were immersed in distilled water for the absorption process, while for the desorption part the specimens were kept at a relative humidity of less than 4 % using a box containing dried silica gel powder (see Fig. 3b).

3.4. Experimental tests

Two types of tests were performed during this research: gravimetrical and tensile tests. In the gravimetrical measurements the square specimens were weighed using AB204-S electronic analytical balance (Mettler Toledo, Switzerland) with a precision of 0.0001 g at specific aging time intervals. The gravimetrical tests were performed repeatedly during the cyclic aging and the final continuous moisture absorption as well and subsequently, the moisture diffusion coefficients were calculated based on Fick's law (Eq. (5)). For the gravimetrical analysis, five samples were manufactured and tested for each aging condition.

For the tensile tests, a Zwick tensile test machine equipped with a 100 N load cell (with the precision of 0.5 %) was used. Dogbone specimens were tested under a constant displacement rate of 1 mm/min. These experimental tests were performed at laboratory conditions (23 °C, 35 % RH). For the tensile experiments, three repetitions were performed for each condition. In order to measure the displacement and strain of the specimens during the tensile tests, a digital image correlation (DIC) setup was used. The experimental setup of the tensile tests is illustrated in Fig. 4.

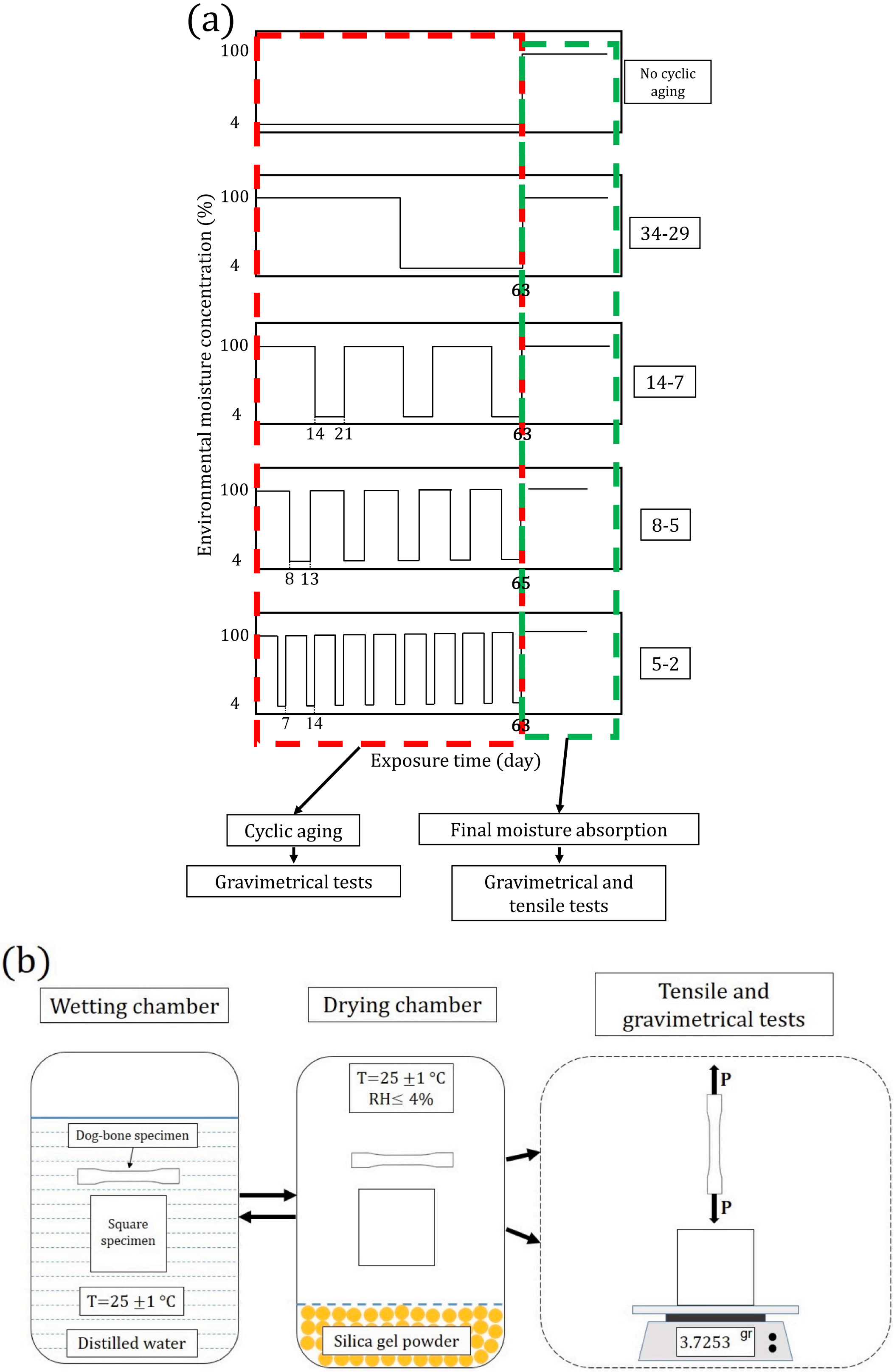

Fig. 3. Aging cycles and exposure times (a), and schematic representation of the aging conditions (b).

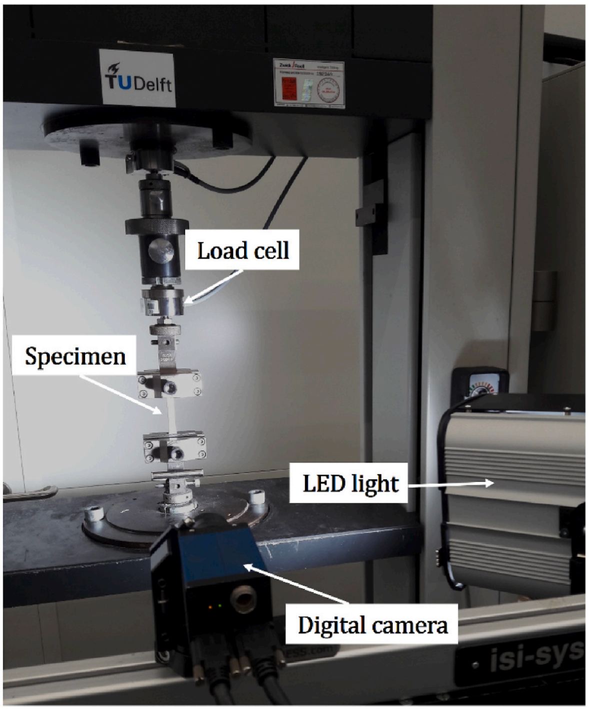

Fig. 4. Tensile test setup.

4. Moisture distribution simulation

Moisture distribution inside the dogbone specimens was simulated using a Finite Element Method (FEM) during the cyclic aging and final moisture absorption. For this purpose, the obtained moisture diffusion coefficients were subsequently utilized in numerical simulations to predict water uptake in dogbone specimens. The aim of numerical simulation is to establish a correlation between the mechanical properties of aged dogbones and their corresponding levels of aging. During simulation process, the moisture diffusion constants measured from Fick's law equation (Eq. (5)) were defined as the material diffusion property. For the first absorption process the specimen was considered completely dry. During the aging cycles, a small amount of water always remains inside the sample after each aging cycle, which should be taken into account in the numerical simulation in order to define the boundary conditions correctly. The numerical simulation was carried out using Abaqus software. 8-node quadratic heat transfer or mass diffusion quadrilateral brick (DC2D8) elements were employed to model the sample behaviour. The most suitable element size was obtained based on the experimental and numerical moisture content comparison which is 0.02 mm. Overall, a total of 20000 elements were created in the

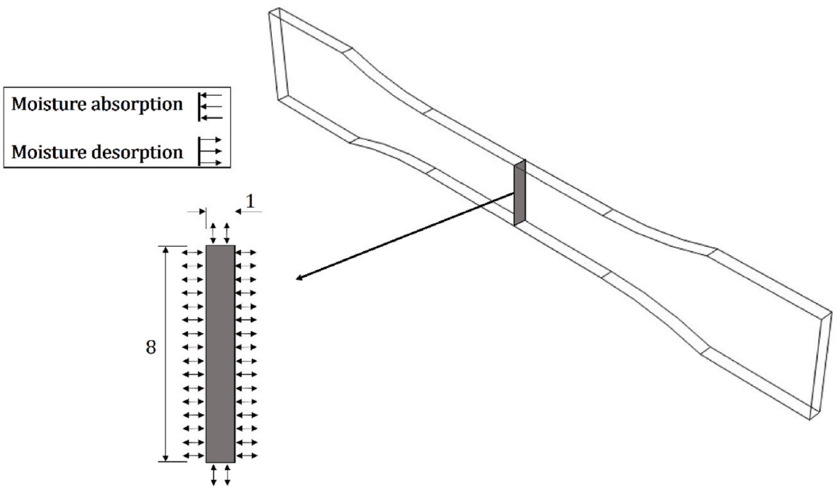

Fig. 5. Schematic of the simulated dog-bone specimen and boundary conditions (dimensions in mm).

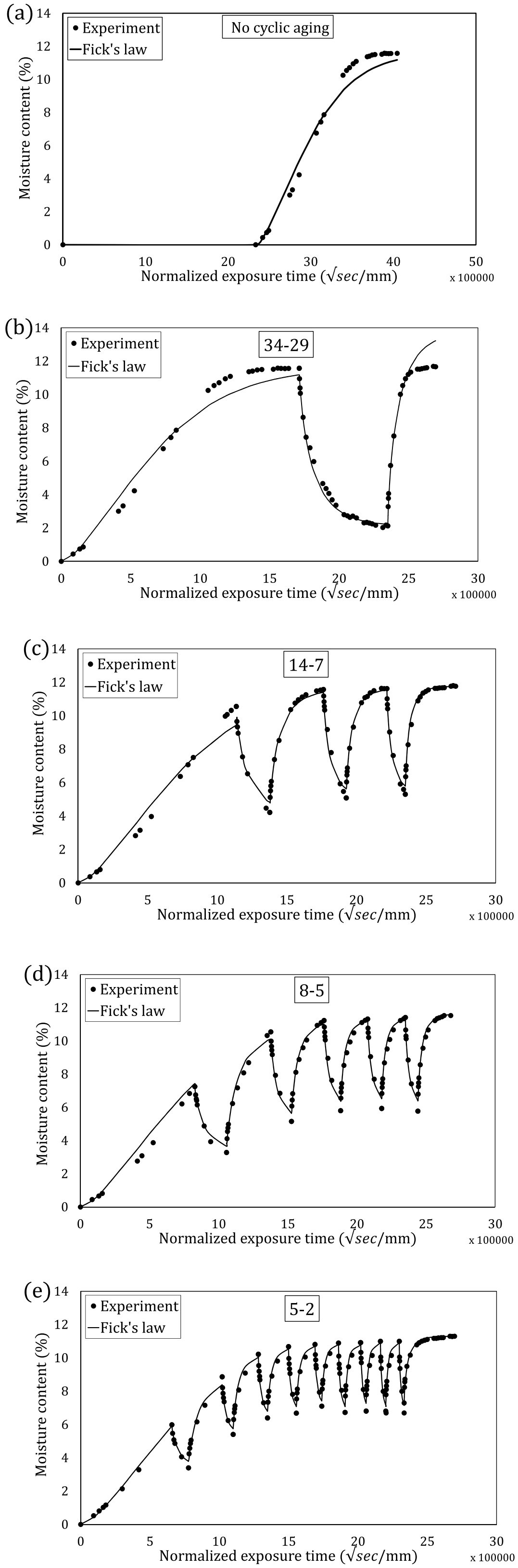

Fig. 6. Experimental and Fick's law curves for specimens without (a), and with 34-29 (b), 14-7 (c), 8-5 (d) and 5-2 (e) cyclic aging.

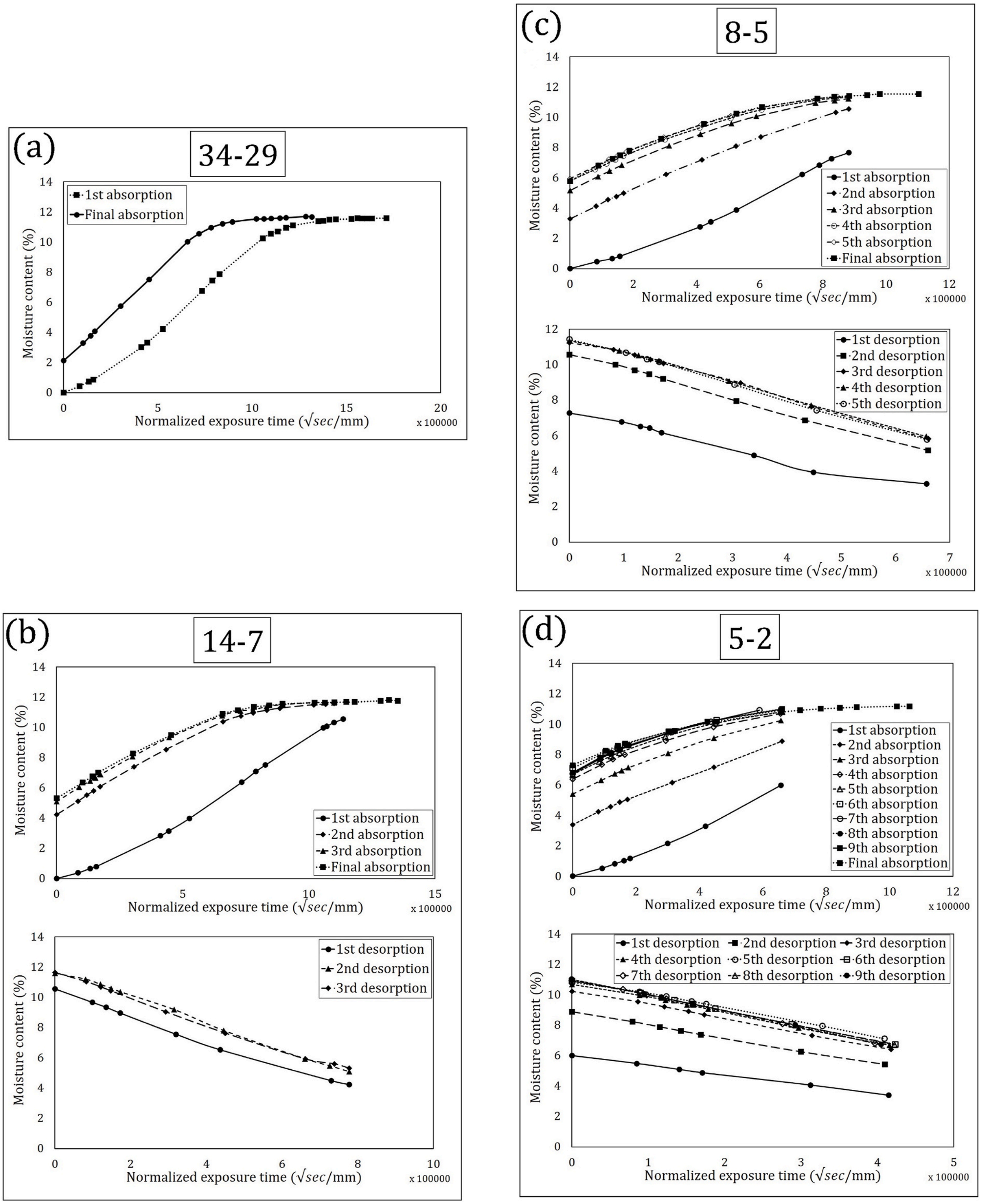

Fig. 7. Experimental moisture absorption and desorption curves for specimens with 34-29 (a), 14-7 (b), 8-5 (c) and 5-2 (d) cyclic aging.

dogbone cross section. Fig. 5 shows the geometry of the simulated dogbone specimen and moisture boundary conditions.

5. Results and discussions

5.1. Moisture absorption-desorption characteristic

Fig. 6 shows the experimental (average of 5 specimens) and Fick's law moisture uptake curves during the cyclic aging process and the final continuous moisture absorption procedure of the gravimetrical specimens.

The comparison of the experimental and Fick's law results shows a good agreement between the curves especially after the first absorption (see Fig. 6). Hence, it can be concluded that the moisture uptake in Araldite 2011 adhesive is Fickian. As can be seen in Fig. 6, in the cyclic aging process 34-29, the adhesive reached the saturation condition at the end of the first moisture absorption

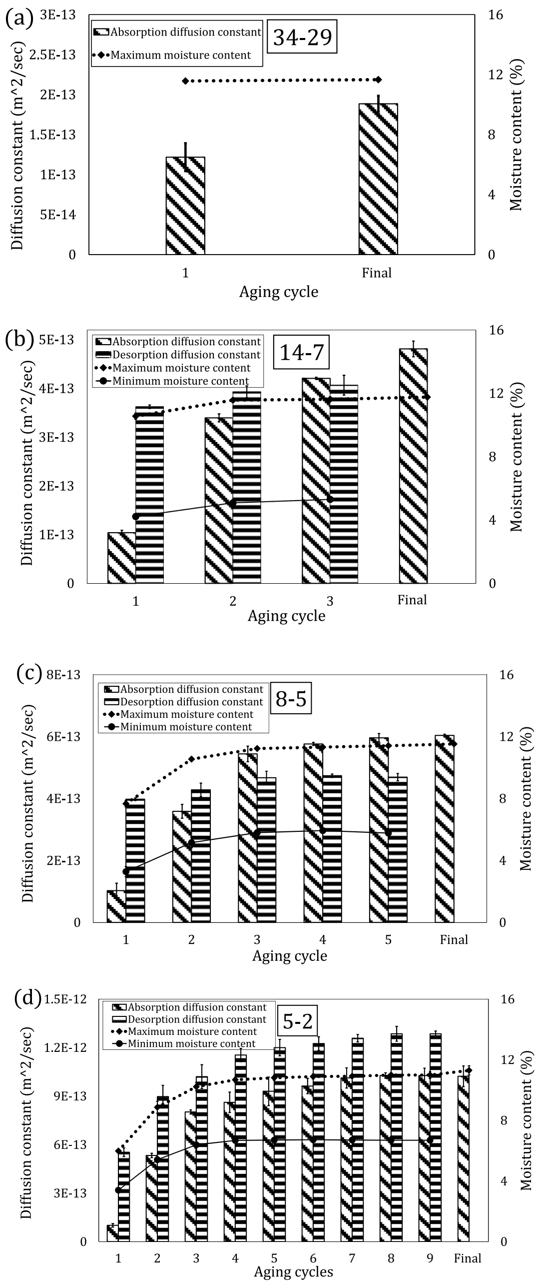

Fig. 8. Moisture diffusion constant and maximum/minimum moisture contents in different aging cycles of 34-29 (a), 14-7 (b), 8-5 (c) and 5-2 (d) cyclic aging.

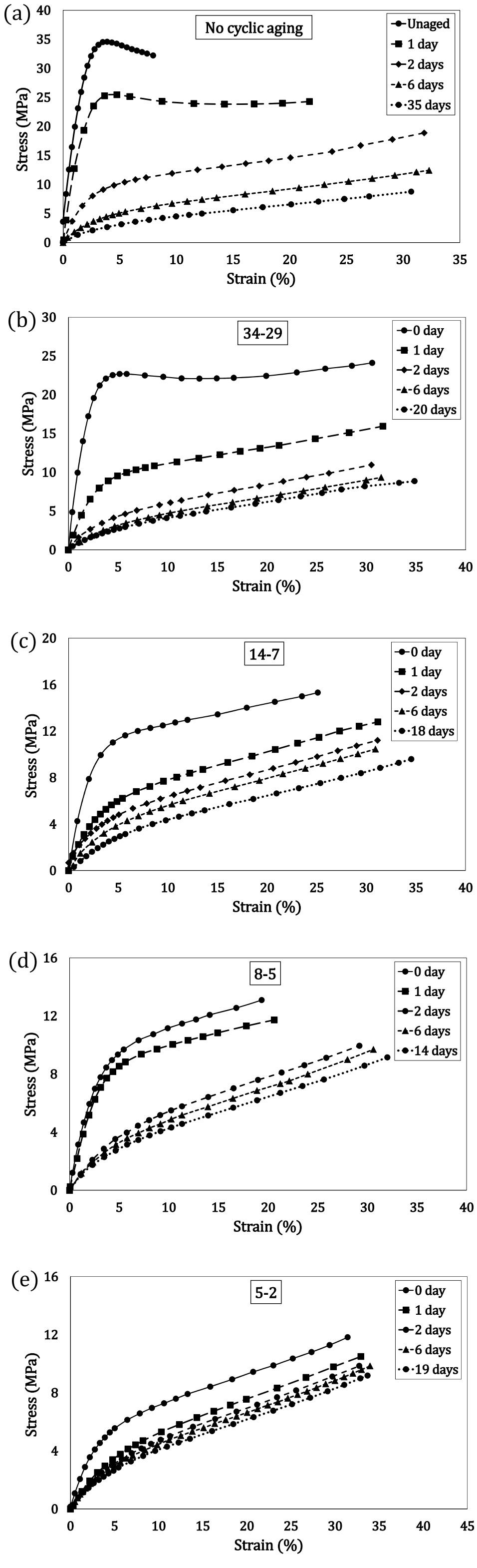

Fig. 9. Stress-strain curves after (a) no cyclic aging (a), after 34-29 (b), 14-7 (c), 8-5 (d) and 5-2 (e) cyclic aging, followed by continuous aging at different exposure times.

process (after 34 days). Afterwards, it dried completely at the end of the desorption process (after 29 days). In the remaining 3 cyclic aging conditions, the specimens did not saturate during the aging cycles.

In order to compare the absorption and desorption curves in different aging cycles, these curves are represented separately in different aging cycles. The experimental results for different cyclic aging frequencies are shown in Fig. 7.

As shown in Fig. 7a, in the 34-29 process, the specimen in final absorption reaches the saturation condition faster than during the 1st absorption. The comparison of moisture absorption curves in Fig. 7b shows that, in 14-7 cyclic aging, the moisture absorption in the 1st absorption is completely different from others; on the contrary, the moisture absorption curves in the 2nd, 3rd, and final absorption curves are similar. The most important reason for this difference between the 1st and other absorption processes is the difference in initial moisture content. On the other hand, as shown in Fig. 7b, the comparison of desorption curves show that they are close together (especially after the 1st cycle) and the moisture uptakes in the same exposure time of different cycles are almost the same. In 8-5 cyclic aging, the moisture absorption and desorption curves in the 1st and 2nd cycles are different from others, and after the 2nd cycle, the moisture absorption and desorption curves are very close to each other (see Fig. 7c). In 5-2 cyclic aging, the moisture absorption and desorption curves in the 1st, 2nd and 3rd cycles are completely different from others, and after the 3rd cycle, the moisture absorption and desorption curves are almost the same (see Fig. 7d).

In general, the moisture absorption and desorption curves show that with increasing the aging frequency, the number of the aging cycles where the moisture diffusion curves become similar, increases. For instance, in 14-7 cyclic aging, only the 1st absorption and desorption curves are different from others, but in 5-2 cyclic aging, the curves in the 1st, 2nd and 3rd cycles are different from others. The comparison of the moisture content curves shows that once the specimen reaches the saturation condition at the end of absorption process, the subsequent moisture uptake curves align together.

To study the moisture diffusion parameters in different aging cycles, Fig. 8 shows the moisture diffusion constants and maximum moisture uptake in each aging cycle.

As can be seen in Fig. 8a, in 34-29 cyclic aging, the moisture diffusion constant increases considerably, but the maximum moisture content at the end of the 1st and final absorption are almost the same.

The comparison of moisture diffusion parameters in 14-7 cyclic aging shows that the moisture diffusion constant in the absorption process increases with the number of aging cycles. This parameter triples from the 1st to the 2nd absorption. In addition, in 14-7 cyclic aging, the moisture diffusion coefficient in the desorption process changes smaller than that in the absorption process. As a result, in the 1st and 2nd cycles, the diffusion coefficient of the absorption is smaller than the desorption. However, in the 3rd cycle, diffusion constant in the absorption becomes bigger than that in the desorption process, which is unusual in monotonous moisture diffusion (see Fig. 8b).

Fig. 8c shows that in 8-5 cyclic aging, the moisture diffusion constants change similar to 14-7 cyclic aging. The moisture diffusion constant in final continuous moisture absorption is 6 times larger than in the 1st absorption diffusion. In this cyclic aging the maximum and minimum moisture contents increase between the 1st and 3rd cycles and remain almost constant after the 3rd cycle.

The variation of moisture diffusion constants in different aging cycles in 5-2 cyclic aging are similar to that of other frequencies. The moisture absorption and desorption constant increase 10 and 2 times, respectively, during the cyclic aging. In this cyclic aging, the maximum and minimum moisture contents increase between the 1st and 4th cycles and remain almost constant after the 4th cycle. There is an important difference in 5-2 cyclic aging in comparison with other aging cycles. In each cycle, the moisture diffusion constant of absorption is always smaller than the moisture diffusion constant in desorption, which is different for other cyclic aging.

The significant variation in the moisture diffusion coefficients of the absorption process can be the result of the swelling and the changes in the dominant diffusion mechanism during the cyclic aging. During the moisture absorption, some mechanisms such as chemical reaction of water molecules with polymer chains, the diffusion of the free water molecules, and micro-cracking takes place. Diffusion of free water molecules is faster than that of other mechanisms. As a result, when micro-cracking and chemical reactions are the dominant mechanisms during the absorption, the diffusion occurs slowly and moisture diffusion coefficient is small in comparison with the diffusion of free water molecules. In each aging frequency, the increasing of moisture diffusion coefficients, shows that, with increasing the aging cycles, the slow diffusion mechanism (such as: micro-cracking and chemical reaction) decrease and fast diffusion of free water molecules will dominantly take place. Another reason for the significant increase of the moisture diffusion rate is the swelling. Swelling happens during the absorption and does not recover completely during the desorption process. Therefore, the moisture absorption will take place faster during the next absorption process.

5.2. *Stress-strain curves after different cyclic aging*

Tensile tests were carried out on dogbone specimens subjected to the cyclic aging followed by continuous aging at different exposure times. The obtained stress-strain curves are shown in Fig. 9. With the exception of Fig. 9a which shows the results for samples subjected to continuous aging. The other results shown in Fig. 9 correspond to samples subjected to cyclic aging followed by continuous aging.

As shown in Fig. 9 during the final continuous moisture absorption, the tensile strength and elastic modulus decrease and the maximum elongation increases with the exposure time. With the increase of the aging frequency the elastic modulus reduces and the tensile strength decreases. The 34-29 cyclic aging leads to a considerable reduction in these parameters while in the 5-2 cyclic aging, the stress-strain curves are close together. However, the most significant reduction of elastic modulus and tensile strength can be observed in joints with no cyclic aging condition.

Fig. 10 shows the variation of elastic modulus and tensile strength of specimens subjected to cyclic aging followed by a continuous aging.

Looking at the results in “0 day” exposure time it can be observed that, the elastic modulus and tensile strength of specimens that experienced cyclic aging are smaller than without cyclic aging. The results obtained after 1 day exposure time in continuous moisture absorption (1 day column) show that with increasing cyclic aging frequencies, the elastic modulus and tensile strength decrease. With increasing exposure time and moisture content (2 days and 6 days), the elastic modulus and tensile strength of specimens decrease continuously and the most significant drop in tensile properties can be found in specimens without cyclic aging. In the saturation condition, the tensile properties (including elastic modulus and tensile strength) of different aging cyclic frequencies approaches together. It means that, with the increase of moisture content, the sensitivity of elastic modulus and tensile strength to the aging frequency decreases during the final moisture uptake. In order to investigate the variation of elastic modulus and tensile strength as a function of moisture content in different aging frequencies, moisture distribution should be simulated during the final moisture absorption for different specimens. This process is reported in the next section.

5.3. Numerical simulation

Based on the parameters obtained experimentally, such as the moisture diffusion constant (D), the moisture distribution in a section of the dogbone specimen was simulated during the cyclic aging and the final continuous moisture absorption. Fig. 11 represents the moisture distribution in dogbone specimens during the final moisture absorption process for different specimens after cyclic aging. It should be mentioned that to account for the residual moisture content from the cyclic aging, the moisture distribution at the end of the cyclic aging phase was considered as the initial moisture content for the second aging phase, which was a continuous aging process.

According to Fig. 11, the initial moisture content remained from cyclic aging (0-day exposure time), the moisture content increased with the cyclic aging frequency, which was observed similarly in the experimental section (see Fig. 8). Fig. 12 shows the variation of moisture content during the final moisture absorption process and after the cyclic aging with different aging frequencies.

The comparison of moisture content during the final moisture absorption process shows that in the same exposure time of final absorption, the moisture contents are completely different, which is due to difference in initial moisture uptake and the moisture diffusion constant. In 14-7, 8-5 and 5-2 cyclic aging the moisture content curves approach each other. From Fig. 12 it can be concluded that in all moisture uptake curves the moisture content increases linearly between 0 and 2 days and after that the moisture absorption rates decrease with increasing exposure times.

The simulated moisture contents during the final moisture absorption process were used in order to study the variation of elastic modulus and tensile strength of the adhesive as a function of moisture content. Fig. 13 illustrates the variation of elastic modulus and tensile strength as a function of moisture content during the final moisture absorption process after the cyclic aging processes.

As can be seen in Fig. 13 the elastic modulus and tensile strength of the specimens change strongly as a function of moisture content during the final absorption process. In addition, the curves of different aging cycles tend to coincide with each other. The comparison of

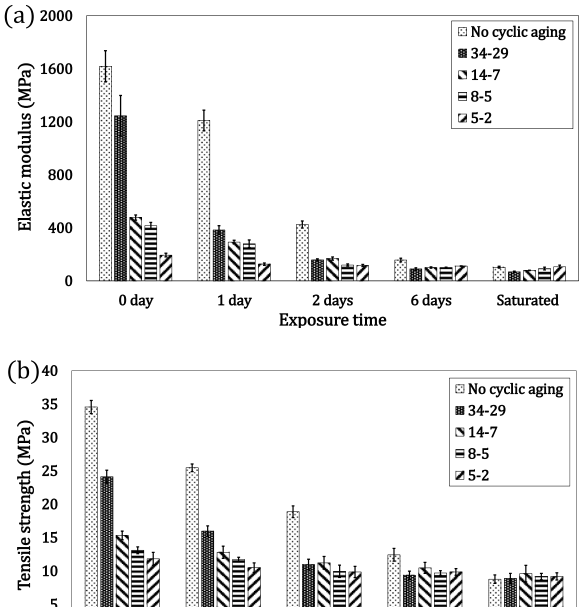

Fig. 10. Variation of elastic modulus (a) and tensile strength (b) during the final continuous moisture absorption after different cyclic aging.

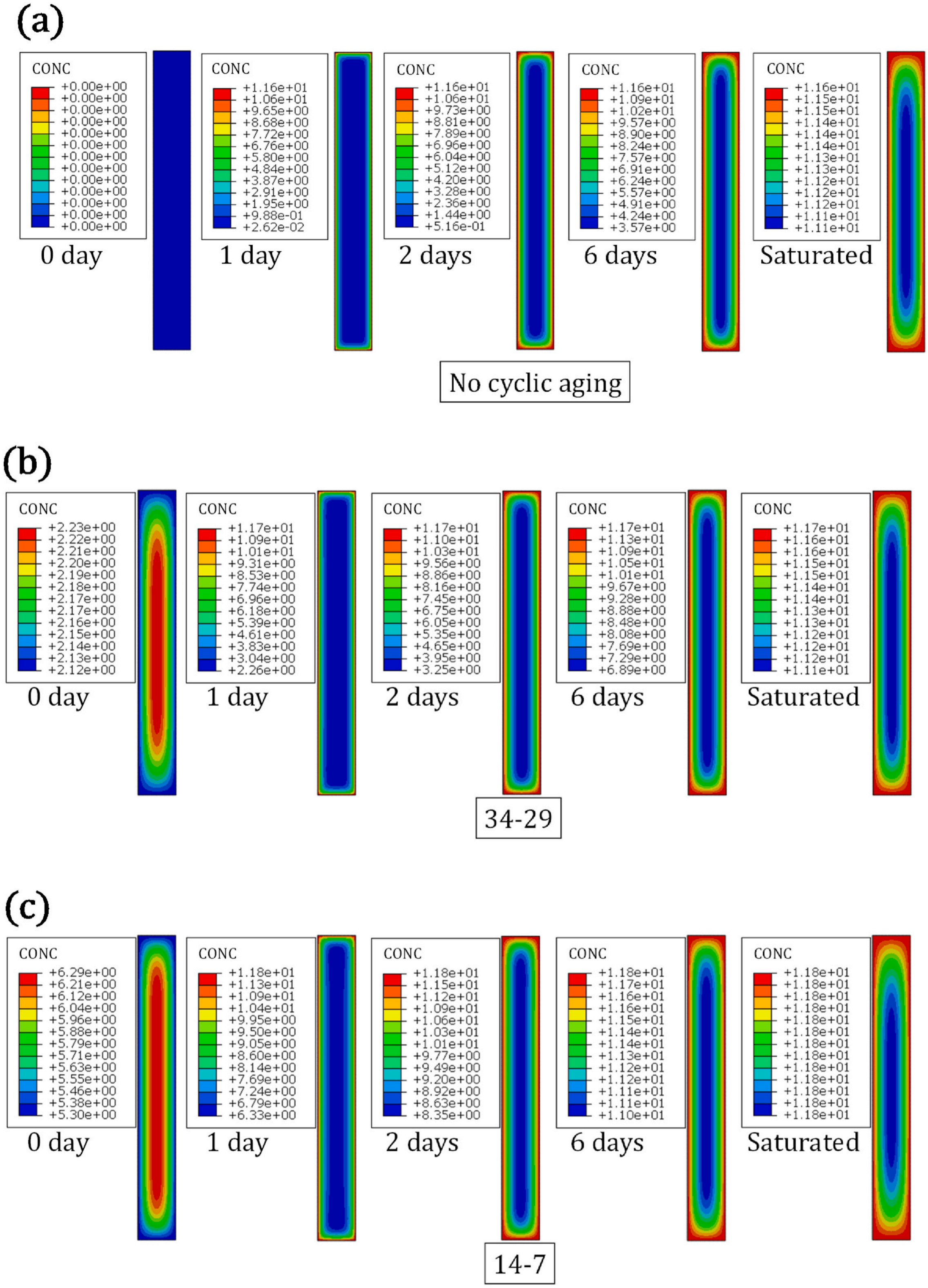

Fig. 11. Simulated moisture distribution during the final moisture absorption process without cyclic aging (a), after 34-29 (b), 14-7 (c), 8-5 (d) and 5-2 (e) cyclic aging (CONC=Moisture concentration).

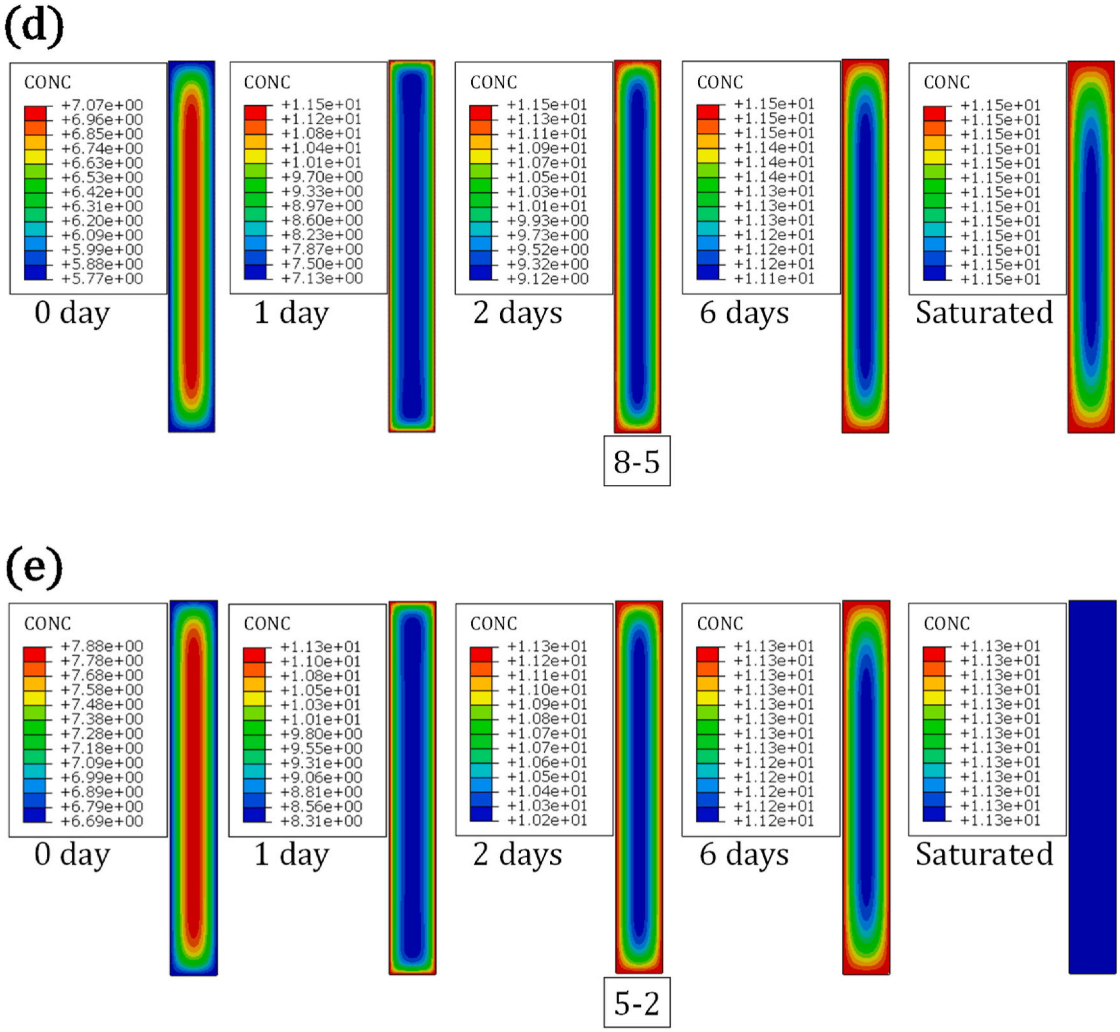

Fig. 11. (*continued*).

experimental results from different cyclic aging conditions shows that these parameters are not sensitive to cyclic aging frequencies in relation to most of the moisture contents. In other words, the variation of the tensile strength as a function of moisture content is similar for different cyclic aging processes (see Fig. 13b). But in case of elastic modulus there is considerable difference in 14-7 and 8-5 cyclic aging in comparison with other cyclic aging processes (see Fig. 13a).

The experimental design, involving bulk specimens exposed to cyclic aging conditions with different frequencies, closely simulates the practical scenarios experienced by adhesive joints in marine structures. This realistic approach enhances the relevance of the study to actual service conditions. The findings contribute valuable insights into the behaviour of epoxy adhesive under cyclic aging conditions, emphasizing the importance of considering aging frequency in the assessment of moisture diffusion and mechanical properties. This information has direct implications for the design and performance evaluation of adhesive joints in marine structures. Also, the study provides analysis on both the moisture diffusion properties and mechanical behaviour of the adhesive. This dual focus enriches the understanding of how cyclic aging frequency influences not only the material's moisture. However, it should be noted that this research has focused exclusively on distilled water. The potential impact of saltwater needs to be explored in future studies. Also the investigation centered on bulk specimens. Subsequent research is required delve into joint ageing, considering factors like substrate effects and interfacial cyclic aging.

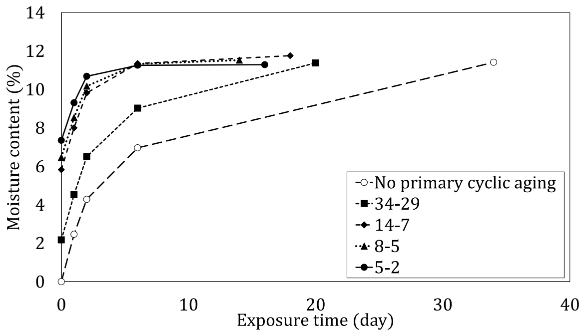

Fig. 12. Simulated moisture content during the final moisture absorption process after different cyclic aging.

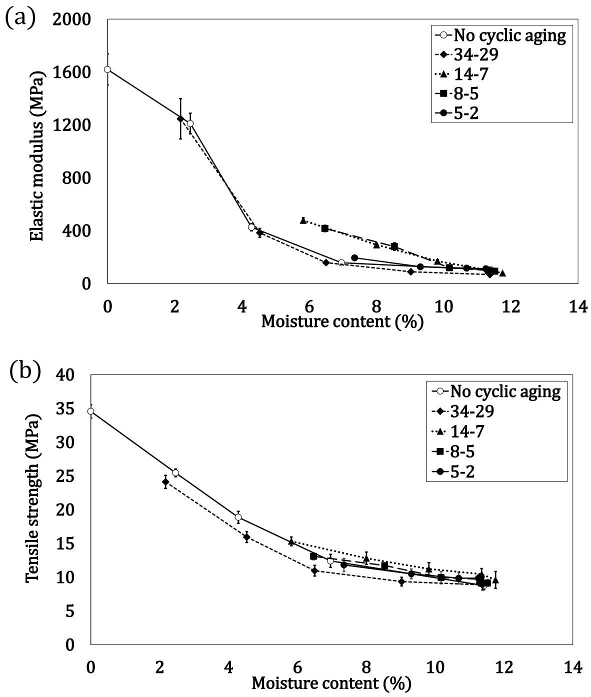

Fig. 13. Variation of the elastic modulus (a) and tensile strength (b) during the final continuous moisture absorption process after different cyclic aging processes.

6. Conclusion

In this paper, the mechanical and moisture diffusion properties of an epoxy adhesive after cyclic aging conditions under different moisture exposure frequencies were investigated.

Based on the obtained results, the following conclusions can be drawn:

- Throughout cyclic aging at all frequencies, the moisture diffusion parameters (diffusion constant and final moisture content) increase with aging cycles.
- Comparative analysis of moisture diffusion variation in different aging cycles reveals a higher rate of increase in the moisture diffusion constant during the absorption process than the desorption process.
- At all aging frequencies, as aging cycles increase, the moisture uptake curves converge. Initial cycles exhibit different curves, becoming similar after the second cycle.
- The reduction in mechanical properties of specimens during the final moisture absorption process diminishes with an increase in cyclic aging frequency, indicating insignificant reduction in high-frequency cyclic aging.
- Across all aging frequencies, during the final moisture absorption process, the elastic modulus and tensile strength gradually decrease in specimens with moisture content exceeding 6 % for the tested adhesive.

- Future studies should investigate the potential impact of saltwater. Further research is needed to explore joint aging, considering factors such as substrate effects and interfacial cyclic aging.

CRediT authorship contribution statement

M. Moazzami: Formal analysis, Investigation, Methodology, Project administration, Software, Validation, Visualization, Writing – original draft. **A. Akhavan-Safar:** Investigation, Methodology, Project administration, Resources, Software, Supervision, Validation, Writing – review & editing. **M.R. Ayatollahi:** Funding acquisition, Investigation, Methodology, Project administration, Resources, Supervision. **Johannes.A. Poulis:** Investigation, Methodology, Software, Supervision. **L.F.M. da Silva:** Supervision, Writing – review & editing. **S. Teixeira De Freitas:** Methodology, Software, Supervision, Validation, Visualization, Writing – review & editing.

Declaration of competing interest

The authors declare that they have no known competing financial interests or personal relationships that could have appeared to influence the work reported in this paper.

Data availability

Data will be made available on request.

References

[1] Da Silva LF, Sato C. Design of adhesive joints under humid conditions. Springer; 2013.

[2] Fernandes P, Viana G, Carbas R, Costa M, da Silva L, Banea M. The influence of water on the fracture envelope of an adhesive joint. Theor Appl Fract Mech 2017;89:1–15.

[3] Delzendehrooy F, Akhavan-Safar A, Barbosa A, Carbas R, Marques E, da Silva L. Investigation of the mechanical performance of hybrid bolted-bonded joints subjected to different ageing conditions: effect of geometrical parameters and bolt size. Journal of Advanced Joining Processes 2022;5:100098.

[4] Dos Reis M, Marques E, Carbas R, Da Silva L. Functionally graded adherends in adhesive joints: an overview. Journal of Advanced Joining Processes 2020;2:100033.

[5] Dubelley F, Planes E, Bas C, Pons E, Yrieix B, Flandin L. The hygrothermal degradation of PET in laminated multilayer. Eur Polym J 2017;87:1–13.

[6] Momber A, Fröck L, Marquardt T. Effects of adhesive type on the mechanical properties of adhesive joints between polyurethane top coats and polyurethane-based adhesives after accelerated atmospheric ageing. Mar Struct 2021;79:103022.

[7] Moazzami M, Ayatollahi MR, Akhavan-Safar A, Teixeira De Freitas S, Poulis JA, da Silva LF. Influence of cyclic aging on adhesive mode mixity in dissimilar composite/metal double cantilever beam joints. Proc Inst Mech Eng Part L 2022:14644207221074696.

[8] Gupta M, Deep V. Effect of water absorption and stacking sequences on the properties of hybrid sisal/glass fibre reinforced polyester composite. Proc Inst Mech Eng Part L 2019;233(10):2045–56.

[9] Pantaloni D, Melelli A, Shah DU, Baley C, Bourmaud A. Influence of water ageing on the mechanical properties of flax/PLA non-woven composites. Polym Degrad Stabil 2022;200:109957.

[10] Sugiman S, Salman S, Anshari B. Hydrothermal ageing of hydrophobic nano-calcium carbonate/epoxy nanocomposites. Polym Degrad Stabil 2021;191:109671.

[11] Ortega-Iguña M, Akhavan-Safar A, Carbas R, Sánchez-Amaya J, Chludzinski M, da Silva L. Use of seawater to improve the static strength and fatigue life of bonded coated steel joints. Polym Degrad Stabil 2022:110169.

[12] Safaei S, Ayatollahi M, Akhavan-Safar A, Moazzami M, Da Silva L. Effect of residual strains on the static strength of dissimilar single lap adhesive joints. J Adhes 2021;97(11):1052–71.

[13] Hirulkar N, Jaiswal P, Reis P, Ferreira J. Bending strength of single-lap adhesive joints under hygrothermal aging combined with cyclic thermal shocks. J Adhes 2021;97(5):493–507.

[14] Feng W, Xu F, Xie W, Zang Y, Zhang X. Hygrothermal aging effects on the mechanical behavior of scarf-repaired composite laminates. J Adhes 2020;96(14):1233–57.

[15] Ortega-Iguña M, Akhavan-Safar A, Carbas R, Sánchez-Amaya J, Chludzinski M, da Silva L. Use of seawater to improve the static strength and fatigue life of bonded coated steel joints. Polym Degrad Stabil 2022;206:110169.

[16] Tian J, Li C, Qi X, Xian G. Hygrothermal aging behavior and mechanism of multi-filler reinforced epoxy composites for steel structure coatings. Eur Polym J 2023;184:111780.

[17] Toscano A, Pitarresi G, Scafidi M, Di Filippo M, Spadaro G, Alessi S. Water diffusion and swelling stresses in highly crosslinked epoxy matrices. Polym Degrad Stabil 2016;133:255–63.

[18] Silva L, Tognana S, Salgueiro W. Study of the water absorption and its influence on the Young's modulus in a commercial polyamide. Polym Test 2013;32(1):158–64.

[19] de Oliveira GL, Gomez AJA, Caire M, Vaz MA, da Costa MF. Characterization of seawater and weather aged polyurethane elastomer for bend stiffeners. Polym Test 2017;59:290–5.

[20] Zhou J, Lucas JP. Hygrothermal effects of epoxy resin. Part I: the nature of water in epoxy. Polymer 1999;40(20):5505–12.

[21] Zhou J, Lucas JP. Hygrothermal effects of epoxy resin. Part II: variations of glass transition temperature. Polymer 1999;40(20):5513–22.

[22] Yang B, Huang WM, Li C, Chor JH. Effects of moisture on the glass transition temperature of polyurethane shape memory polymer filled with nano-carbon powder. Eur Polym J 2005;41(5):1123–8.

[23] Brettle J, Brewis D, Comyn J, Cope B, Goosey M, Hurditch R. The interaction of water with an epoxide adhesive based on the diglycidylether of bisphenol-A and triethylene tetramine. Int J Adhesion Adhes 1983;3(4):189–92.

[24] De Nève B, Shanahan M. Effects of humidity on an epoxy adhesive. Int J Adhesion Adhes 1992;12(3):191–6.

[25] Mubashar A, Ashcroft IA, Critchlow GW, Crocombe A. Modelling cyclic moisture uptake in an epoxy adhesive. J Adhes 2009;85(10):711–35.

[26] Bordes M, Davies P, Cognard J-Y, Sohier L, Sauvant-Moynot V, Galy J. Prediction of long term strength of adhesively bonded steel/epoxy joints in sea water. Int J Adhesion Adhes 2009;29(6):595–608.

[27] Mubashar A, Ashcroft IA, Critchlow GW, Crocombe A. Moisture absorption–desorption effects in adhesive joints. Int J Adhesion Adhes 2009;29(8):751–60.

[28] Zanni-Deffarges M, Shanahan M. Diffusion of water into an epoxy adhesive: comparison between bulk behaviour and adhesive joints. Int J Adhesion Adhes 1995;15(3):137–42.

[29] Brewis D, Comyn J, Tegg J. The durability of some epoxide adhesive-bonded joints on exposure to moist warm air. Int J Adhesion Adhes 1980;1(1):35–9.

[30] Liljedahl C, Crocombe A, Wahab M, Ashcroft I. Modelling the environmental degradation of the interface in adhesively bonded joints using a cohesive zone approach. J Adhes 2006;82(11):1061–89.

[31] Bowditch M. The durability of adhesive joints in the presence of water. Int J Adhesion Adhes 1996;16(2):73–9.
[32] Kinloch A, Korenberg C, Tan K. Durability of structural adhesive joints. Applied Sciences Publishers; 1983.
[33] Adams RD. Adhesive bonding: science, technology and applications. Elsevier; 2005.
[34] Viana G, Costa M, Banea M, Da Silva L. A review on the temperature and moisture degradation of adhesive joints. Proc IME J Mater Des Appl 2017;231(5):488–501.
[35] Moazzami M, Ayatollahi M, Akhavan-Safar A, Da Silva L. Experimental and numerical analysis of cyclic aging in an epoxy-based adhesive. Polym Test 2020;91:106789.
[36] Da Costa J, Akhavan-Safar A, Marques E, Carbas R, Da Silva L. Cyclic ageing of adhesive materials. J Adhes 2022;98(10):1341–57.
[37] Moazzami M, Ayatollahi M, Akhavan-Safar A, De Freitas ST, Poulis J, da Silva L. Effect of cyclic aging on mode I fracture energy of dissimilar metal/composite DCB adhesive joints. Eng Fract Mech 2022;271:108675.
[38] Houjou K, Shimamoto K, Akiyama H, Sato C. Effect of cyclic moisture absorption/desorption on the strength of epoxy adhesive joints and moisture diffusion coefficient. J Adhes 2022;98(11):1535–51.
[39] Da Costa J, Akhavan-Safar A, Marques E, Carbas R, Da Silva L. Effects of cyclic ageing on the tensile properties and diffusion coefficients of an epoxy-based adhesive. Proc Inst Mech Eng Part L 2021;235(6):1451–60.
[40] Liu L, Xu K, Xu Y, Zhao Z, Luo G, Chen W. Experimental study of quasi-static and dynamic tensile behavior of epoxy resin under cyclic hygrothermal aging. Polym Degrad Stabil 2022;200:109940.
[41] Crank J. The Mathematics of diffusion. London: Oxford Univ. Press; 1975.
[42] Costa M, et al. Effect of the size reduction on the bulk tensile and double cantilever beam specimens used in cohesive zone models. Proc Inst Mech Eng Part L 2016;230(5):968–82.